



Published as: *Science*. 2009 October 2; 326(5949): 144–147.

Genome-Wide RNAi Screen Identifies Letm1 as a Mitochondrial Ca²⁺/H⁺ Antiporter

Dawei Jiang, Linlin Zhao, and David E. Clapham*

Department of Cardiology, Howard Hughes Medical Institute, Children's Hospital Boston, Manton Center for Orphan Disease, and Department of Neurobiology, Harvard Medical School, Enders Building 1309, 320 Longwood Avenue, Boston, MA 02115, USA

Abstract

Mitochondria are integral components of cellular calcium (Ca²⁺) signaling. Calcium stimulates mitochondrial adenosine 5'-triphosphate production, but can also initiate apoptosis. In turn, cytoplasmic Ca²⁺ concentrations are regulated by mitochondria. Although several transporter and ion-channel mechanisms have been measured in mitochondria, the molecules that govern Ca²⁺ movement across the inner mitochondrial membrane are unknown. We searched for genes that regulate mitochondrial Ca²⁺ and H⁺ concentrations using a genome-wide *Drosophila* RNA interference (RNAi) screen. The mammalian homolog of one *Drosophila* gene identified in the screen, *Letm1*, was found to specifically mediate coupled Ca²⁺/H⁺ exchange. RNAi knockdown, overexpression, and liposome reconstitution of the purified Letm1 protein demonstrate that Letm1 is a mitochondrial Ca²⁺/H⁺ antiporter.

Mitochondrial Ca²⁺ uptake across the inner mitochondrial membrane occurs via tightly regulated channels [e.g., MCU/MiCa (1, 2) and transporters (3-6)]. Increases in the concentration of calcium ([Ca²⁺]) in the mitochondrial matrix enhance the activities of adenosine 5'-triphosphate (ATP) synthase and enzymes in the tricarboxylic acid cycle (7, 8), but if homeostatic mechanisms fail, high levels of matrix Ca²⁺ induce cell death (9, 10). We set out to identify the genes that mediate Ca²⁺ flux across the inner mitochondrial membrane.

We conducted a genome-wide, high-throughput RNA interference (RNAi) screen to identify genes that control mitochondrial Ca²⁺ transport. *Drosophila* S2 cells stably expressing mitochondria-targeted ratiometric pericam were incubated with arrayed double-stranded RNAs (dsRNAs) against each of the ~22,000 *Drosophila* genes (11). Mitochondrial (Mt)-pericam emission due to excitation at 405 nm is sensitive to changes in [Ca²⁺], whereas emission in response to excitation at 488 nm independently reports changes in pH (figs. S1 and S2). Through a series of screens discussed in the supporting online material (SOM) (fig.

*To whom correspondence should be addressed. dclapham@enders.tch.harvard.edu.

Supporting Online Material

www.sciencemag.org/cgi/content/full/326/5949/144/DC1

SOM Text

Materials and Methods

Figs. S1 to S9

Tables S1 to S3

S2 and tables S1 to S3), *CG4589*, the *Drosophila* homolog of the human gene *Letm1*, was identified as a gene strongly affecting $[Ca^{2+}]_{mito}$ and $[H^+]_{mito}$ responses. Mammalian uncoupling proteins (UCPs) were recently proposed to be critical for Ca^{2+}_{mito} uptake (12) [but see (13)]. However, dsRNAs against *Drosophila* mitochondrial UCPs did not affect $[Ca^{2+}]_{mito}$ and $[H^+]_{mito}$ changes in our screen and subsequent assays (fig. S4).

Extramitochondrial $[Ca^{2+}]$ was clamped in permeabilized S2 cells in Na^+ -free intracellular solution to abrogate potential mitochondrial Na^+ ($/H^+$ or $/Ca^{2+}$) exchangers. Basal $[Ca^{2+}]_{mito}$ and $[H^+]_{mito}$ were similar in control and dLetm1 knockdown cells under this condition (fig. S5). dLetm1 knockdown markedly reduced Ca^{2+}_{mito} uptake at $<1 \mu M$ $[Ca^{2+}]_{cyto}$, a transport mode coupled with mitochondrial H^+ extrusion (Fig. 1A). Free $[Ca^{2+}]_{mito}$ at steady state was $\sim 5 \mu M$, far below the calculated free $[Ca^{2+}]_{mito}$ equilibrium ($\sim 1 M$, assuming $1 \mu M$ cytoplasmic $[Ca^{2+}]$), indicating an intrinsic limit for this mode of uptake. At $[Ca^{2+}]_{cyto} > 1 \mu M$, a dLetm1-independent Ca^{2+}_{mito} uptake mode became apparent (Fig. 1B). This rapid Ca^{2+}_{mito} uptake mode stimulated by higher $[Ca^{2+}]_{cyto}$ was not associated with H^+ extrusion and caused membrane depolarization, consistent with MCU/MiCa. dLetm1 knockdown had little effect on $100 \mu M$ $[Ca^{2+}]_{cyto}$ -induced Ca^{2+}_{mito} influx (Fig. 1A).

Ca^{2+}_{mito} uptake in cells lacking dLetm1 was not coupled with H^+ extrusion. We measured voltage across the inner mitochondrial membrane (Ψ_{mito}) using tetramethyl rhodamine methyl ester (TMRM; 5 nM) to determine whether dLetm1 knockdown affected electron transport chain (ETC)-dependent proton export. Unlike ETC inhibitors that reduce Ψ_{mito} in control cells, resting Ψ_{mito} was increased in dLetm1-knockdown cells (Fig. 1, C and D). To summarize the results thus far, dLetm1 is crucial to Ca^{2+}_{mito} uptake in low $[Ca^{2+}]$, and the pH gradient appears to intrinsically limit dLetm1-associated mitochondrial Ca^{2+} uptake.

To test the apparent limitation by the pH gradient, we studied pH-dependent changes on $[Ca^{2+}]_{mito}$ and $[H^+]_{mito}$. Ca^{2+}_{mito} extrusion and H^+ influx were induced by a decline in $[Ca^{2+}]_{cyto}$, and by cytoplasmic acidification (Fig. 1E). dLetm1 knockdown specifically abolished Ca^{2+} -dependent pH changes and pH-driven Ca^{2+}_{mito} extrusion. As expected, alkalization induced an initial phase of rapid Ca^{2+}_{mito} uptake and H^+ extrusion, and a much slower second phase of Ca^{2+}_{mito} uptake and H^+ extrusion (Fig. 1F). The pH-dependent Ca^{2+}_{mito} uptake was slowed by more than fourfold in dLetm1 knockdown cells. In the yeast *mdm38* (homolog of *Letm1* and *CG4589*) mutant, mitochondria were swollen and the phenotype could be rescued by the exogenous K^+/H^+ exchanger, nigericin (14). In these studies, however, active mitochondrial K^+/H^+ exchange was only observed under low-divalent or divalent-free conditions (14). In our experiments in dLetm1 knockdown S2 cells, application of nigericin augmented H^+ flux (Fig. 1, E and F), but did not rescue the loss of pH-driven Ca^{2+} exchange.

The human homolog of *CG4589*, *Letm1* (leucine zipper EF-hand-containing transmembrane protein 1), is an evolutionarily conserved, ubiquitously expressed, homomeric inner mitochondrial membrane protein of unclear function (15-18). In humans, partial deletion of the short arm of chromosome 4 (including *Letm1*) results in Wolf-Hirschhorn syndrome (WHS), characterized by mental retardation, microcephaly, seizures, hypotonia, and cleft

lip/palate (19). In mammalian cells, Cherry-tagged Letm1 was exclusively localized to the mitochondrial inner membrane (Fig. 2, A and B). In cells overexpressing Letm1, pH-driven $\text{Ca}^{2+}_{\text{mito}}$ uptake and $\text{H}^{+}_{\text{mito}}$ extrusion were accelerated by more than fivefold (Fig. 2C). Mitochondrial H^{+} transport was not secondary to $[\text{Ca}^{2+}]_{\text{mito}}$ alone, but rather to the Ca^{2+} gradient across the inner mitochondrial membrane (fig. S6).

Most HeLa cells with short-term (~3 days) *Letm1* small interfering RNA (siRNA) treatment appeared healthy and their mitochondria appeared normal under light microscopy (Fig. 3A), despite an ~70% reduction in mRNA level (Fig. 3B). Knockdown of Letm1 abolished bidirectional mitochondrial $\text{Ca}^{2+}/\text{H}^{+}$ antiport, resulting in reduced initial $\text{Ca}^{2+}_{\text{mito}}$ uptake and late $\text{Ca}^{2+}_{\text{mito}}$ overload (Fig. 3, C and D), supporting the essential role of Letm1 in $\text{Ca}^{2+}/\text{H}^{+}$ antiporter function and $[\text{Ca}^{2+}]_{\text{mito}}$ homeostasis. As in S2 cells, knockdown of Letm1 did not cause a decrease, but rather a slight increase, in resting Ψ_{mito} (fig. S7), consistent with a previous report that Letm1 knockdown does not impair ETC function (17).

To directly test whether the Letm1 protein mediates $\text{Ca}^{2+}/\text{H}^{+}$ antiport, C-terminal His-tagged Letm1 was expressed in bacteria, purified (Fig. 4A), and incorporated into liposomes. Letm1-containing liposomes rapidly accumulated Ca^{2+} . Ca^{2+} uptake was blocked by Ruthenium red (and Ru360), nonselective inhibitors of divalent cation channels and transporters (Fig. 4B). CGP-37157 (~4 μM), a nonselective inhibitor of $\text{Na}^{+}/\text{Ca}^{2+}$ exchangers, inhibited the transport rate by ~25%. Addition of Ca^{2+} induced H^{+} efflux; also transiently increasing external pH induced rapid H^{+} efflux from Letm1-liposomes (Fig. 4C). In symmetrical $[\text{Ca}^{2+}]$, external acidic pH drove Ca^{2+} release (Fig. 4D), whereas alkaline pH induced Ca^{2+} uptake (Fig. 4E). The maximum rate of Ca^{2+} transport (V_{max}) by isolated Letm1 protein was 4.1 nmol/ μg protein per second [~ 1700 ions per second, assuming that Letm1 is tetrameric (22, 23)], reaching half-saturation at 132.7 nmol $\text{Ca}^{2+}/\mu\text{g}$ protein; Michaelis constant (K_{m}) = 137 nmol $\text{Ca}^{2+}/\mu\text{g}$ protein (Fig. 4F). Ca^{2+} transport velocity was increased about sevenfold by increasing the transliposomal potential (fig. S8), suggesting that Letm1 is electrogenic. These results, using isolated Letm1-containing liposomes, strongly suggest that Letm1 itself comprises a $\text{Ca}^{2+}/\text{H}^{+}$ antiporter.

We showed that Letm1 is a $\text{Ca}^{2+}/\text{H}^{+}$ exchanger in S2 cells, mammalian cells, and as an isolated protein in proteoliposomes. Letm1 exchanges Ca^{2+} for H^{+} at submicromolar $[\text{Ca}^{2+}]_{\text{cyto}}$. When $[\text{Ca}^{2+}]_{\text{mito}}$ is high, such as after MCU/MiCa activation, or when cytoplasmic pH is low, Letm1 should extrude excess Ca^{2+} and acidify the mitochondrial matrix. When $[\text{Ca}^{2+}]_{\text{mito}}$ is low, Ca^{2+} will be imported and the mitochondrial matrix alkalized. Letm1 $\text{Ca}^{2+}/\text{H}^{+}$ exchange was not sensitive to $[\text{Na}^{+}]$. Prior evidence for Na^{+} -dependent Ca^{2+} extrusion suggests that a third molecule, probably a $\text{Na}^{+}/\text{Ca}^{2+}$ exchanger, is also present in the inner mitochondrial membrane (1, 4, 5). We speculate that the relative amounts of these three Ca^{2+} -exchange mechanisms vary in different cell types, correlating with their cell-specific functions.

We found that long-term Letm1 knockdown with repetitive siRNA application resulted in morphological changes in certain HeLa cell subpopulations (~20% cells). However, other studies showed no mitochondrial morphology changes in lymphoblastoid cells and primary fibroblasts from WHS patients despite a notable reduction in the amount of Letm1 protein

(17). These data suggest that mitochondrial morphology changes are secondary to the loss of Letm1, but may depend on cell type.

Letm1 has no appreciable homology to the bacterial and plant CaX family of Ca²⁺/H⁺ or Ca²⁺/Na⁺ transporters. Based on our preliminary analysis of the potential topologies using *Robetta* (fig. S9) (20), we hypothesize that Letm1 resembles the inner mitochondrial membrane Mg²⁺ transporter (21), whose bacterial homolog (CorA) forms a funnel-shaped structure (22, 23).

Supplementary Material

Refer to Web version on PubMed Central for supplementary material.

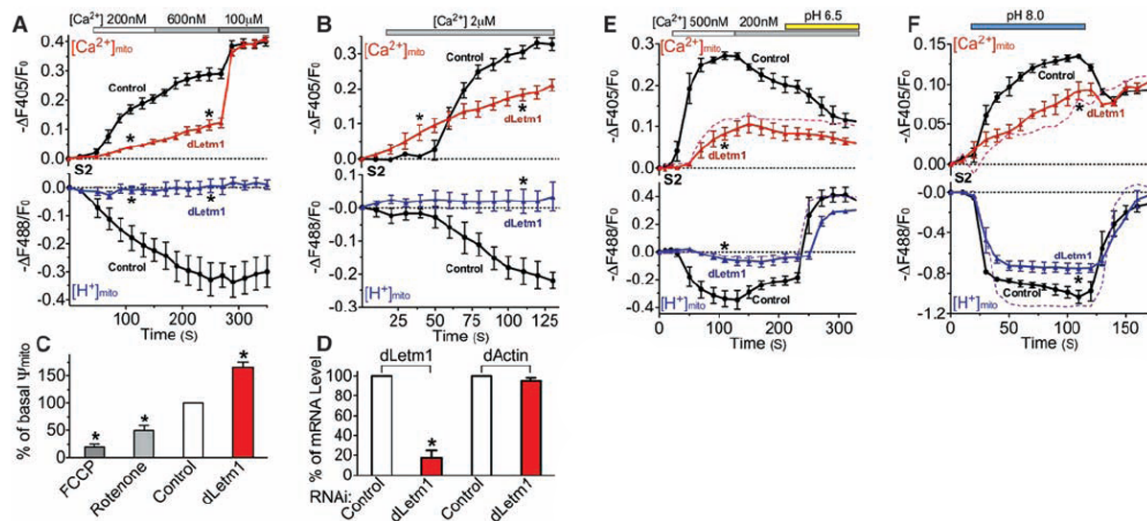
Acknowledgments

We thank B. Mathey-Prevot, N. Ramadan, M. Booker, and staff at the Drosophila RNAi Screening Center for assistance with the screen; A. Miyawaki for pericam; R. Tsien for CherryFP; T. Schwarz for the PMK33 vector; R. Kaplan for advice on the proteoliposome study; D. Baker for assistance with *Robetta*; and G. Krapivinsky, Y. Kirichok, and J. Jin for discussions. D.J. is a recipient of fellowship awards from the Canadian Institutes of Health Research and the Alberta Heritage Foundation for Medical Research.

References and Notes

1. Rizzuto R, Bernardi P, Pozzan T. *J Physiol.* 2000; 529:37. [PubMed: 11080249]
2. Kirichok Y, Krapivinsky G, Clapham DE. *Nature.* 2004; 427:360. [PubMed: 14737170]
3. Gunter KK, Gunter TE. *J Bioenerg Biomembr.* 1994; 26:471. [PubMed: 7896763]
4. Bernardi P. *Physiol Rev.* 1999; 79:1127. [PubMed: 10508231]
5. Demaurex N, Poburko D, Frieden M. *Biochim Biophys Acta.* 2009; 1787:1383. [PubMed: 19161976]
6. Nicholls DG. *Biochim Biophys Acta.* 2008; 1777:550. [PubMed: 18423395]
7. Szabadkai G, Duchon MR. *Physiology (Bethesda).* 2008; 23:84. [PubMed: 18400691]
8. Hajnoczky G, Robb-Gaspers LD, Seitz MB, Thomas AP. *Cell.* 1995; 82:415. [PubMed: 7634331]
9. Rasola A, Bernardi P. *Apoptosis.* 2007; 12:815. [PubMed: 17294078]
10. Giacomello M, Drago I, Pizzo P, Pozzan T. *Cell Death Differ.* 2007; 14:1267. [PubMed: 17431419]
11. Ramadan N, Flockhart I, Booker M, Perrimon N, Mathey-Prevot B. *Nat Protocols.* 2007; 2:2245.
12. Trenker M, Malli R, Fertschai I, Levak-Frank S, Graier WF. *Nat Cell Biol.* 2007; 9:445. [PubMed: 17351641]
13. Brookes PS, et al. *Nat Cell Biol.* 2008; 10:1235. [PubMed: 18978830]
14. Nowikovsky K, Reipert S, Devenish RJ, Schweyen RJ. *Cell Death Differ.* 2007; 14:1647. [PubMed: 17541427]
15. Piao L, et al. *Cancer Res.* 2009; 69:3397. [PubMed: 19318571]
16. Tamai S, et al. *J Cell Sci.* 2008; 121:2588. [PubMed: 18628306]
17. Dimmer KS, et al. *Hum Mol Genet.* 2008; 17:201. [PubMed: 17925330]
18. Hasegawa A, van der Blik AM. *Hum Mol Genet.* 2007; 16:2061. [PubMed: 17606466]
19. Bergemann AD, Cole F, Hirschhorn K. *Trends Genet.* 2005; 21:188. [PubMed: 15734578]
20. Kim DE, Chivian D, Baker D. *Nucleic Acids Res.* 2004; 32:W526. [PubMed: 15215442]
21. Schindl R, Weghuber J, Romanin C, Schweyen RJ. *Biophys J.* 2007; 93:3872. [PubMed: 17827224]
22. Lunin VV, et al. *Nature.* 2006; 440:833. [PubMed: 16598263]
23. Eshaghi S, et al. *Science.* 2006; 313:354. [PubMed: 16857941]

24. Materials and methods and references are given in the supporting material available on *Science* Online.

**Fig. 1.**

dLetm1 knockdown reduces Ca^{2+}/H^+ antiport. (A) $[Ca^{2+}]_{mito}$ (upper panel) and $[H^+]_{mito}$ (lower panel) measurements in digitonin-permeabilized S2-pericam cells treated with scrambled control (circles; $n = 6$, 194 cells) or *dLetm1* dsRNAs (triangles; $n = 6$, 167 cells). (B) Experiment as in (A), but with 2 μ M Ca^{2+} applied to cells treated with scrambled control (circles; $n = 4$, 93 cells) or *dLetm1* dsRNAs (triangles; $n = 4$, 81 cells). (C) Transmembrane potential (Ψ_{mito} ; measured with 5 nM TMRM) in control S2-pericam cells was reduced by the ETC inhibitors rotenone and antimycin (5 μ M, $n = 3$, 81 cells) or by the protonophore trifluoromethoxy carbonyl cyanide phenylhydrazine (FCCP; 10 μ M, $n = 3$, 102 cells). By contrast, Ψ_{mito} was increased in *dLetm1* knockdown cells ($n = 3$, 113 cells) as compared to cells treated with scrambled control dsRNA ($n = 3$, 168 cells). (D) Relative mRNA level of *dLetm1* and actin in control and *dLetm1* dsRNA-treated S2 cells by quantitative reverse transcription–polymerase chain reaction (RT-PCR) ($n = 3$). (E) Ca^{2+} - and pH gradient–driven $[Ca^{2+}]_{mito}$ and $[H^+]_{mito}$ changes in permeabilized S2-pericam cells treated with control (circles; $n = 4$, 143 cells) or *dLetm1* dsRNAs (triangles; $n = 4$, 113 cells). A representative trace shows the effect of applying the H^+/K^+ antiporter nigericin (1 μ M, dashed colored line) on *dLetm1* dsRNA-treated cells ($n = 3$, 87 cells). (F) pH-dependent $[Ca^{2+}]_{mito}$ and $[H^+]_{mito}$ changes in permeabilized S2-pericam cells treated with scrambled control (circles; $n = 6$, 214 cells) or *dLetm1* dsRNAs (triangles; $n = 6$, 187 cells). BAPTA-maintained test solution $[Ca^{2+}] = 50$ nM. A representative trace shows the effect of nigericin (1 μ M, dotted line) on *dLetm1* dsRNA-treated cells ($n = 3$, 104 cells). All data shown are the mean \pm SEM (* $P < 0.05$, two-tailed Student's *t* test).

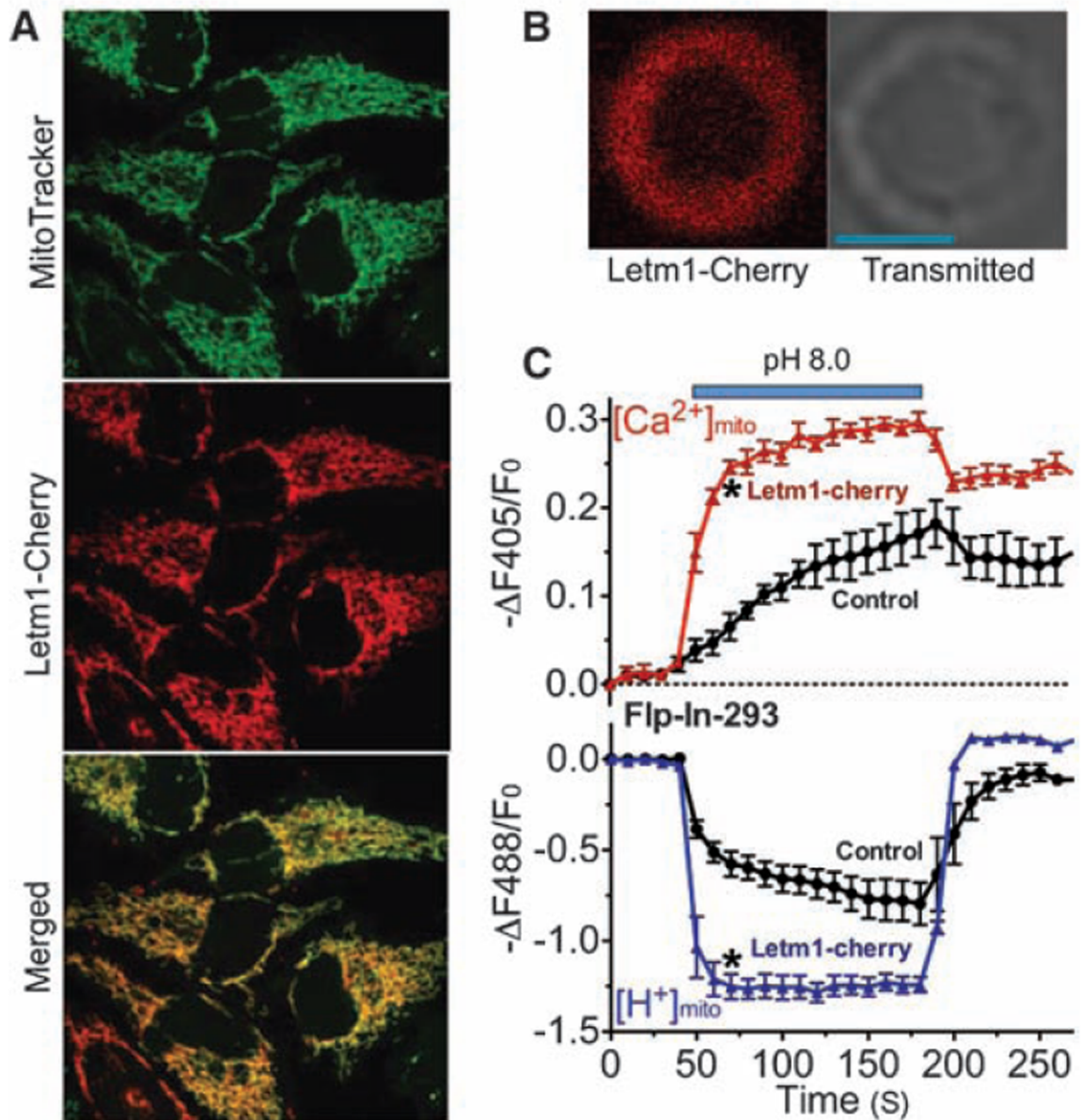


Fig. 2. Letm1 overexpression enhances $\text{Ca}^{2+}/\text{H}^{+}$ antiport. **(A)** Letm1 is localized to mitochondria. Representative images of Flp-In-293-pericam cells transfected with Letm1-Cherry and loaded with 10 nM MitoTracker green. **(B)** Representative image of a Letm1-Cherry-labeled mitoplast; Letm1-Cherry was targeted to the mitochondrial inner membrane. Scale bar: 2 μm . **(C)** Alkaline pH (pH 8.0) increased $[\text{Ca}^{2+}]_{\text{mito}}$ and decreased $[\text{H}^{+}]_{\text{mito}}$ in digitonin-permeabilized Flp-In-293-pericam cells in vector controls (circles; $n = 5$, 119 cells). Overexpression of Letm1-Cherry (triangles; $n = 5$, 93 cells) enhanced these changes. $[\text{Ca}^{2+}]_o = 250$ nM. Data shown are the mean \pm SEM (* $P < 0.05$, two-tailed Student's t test).

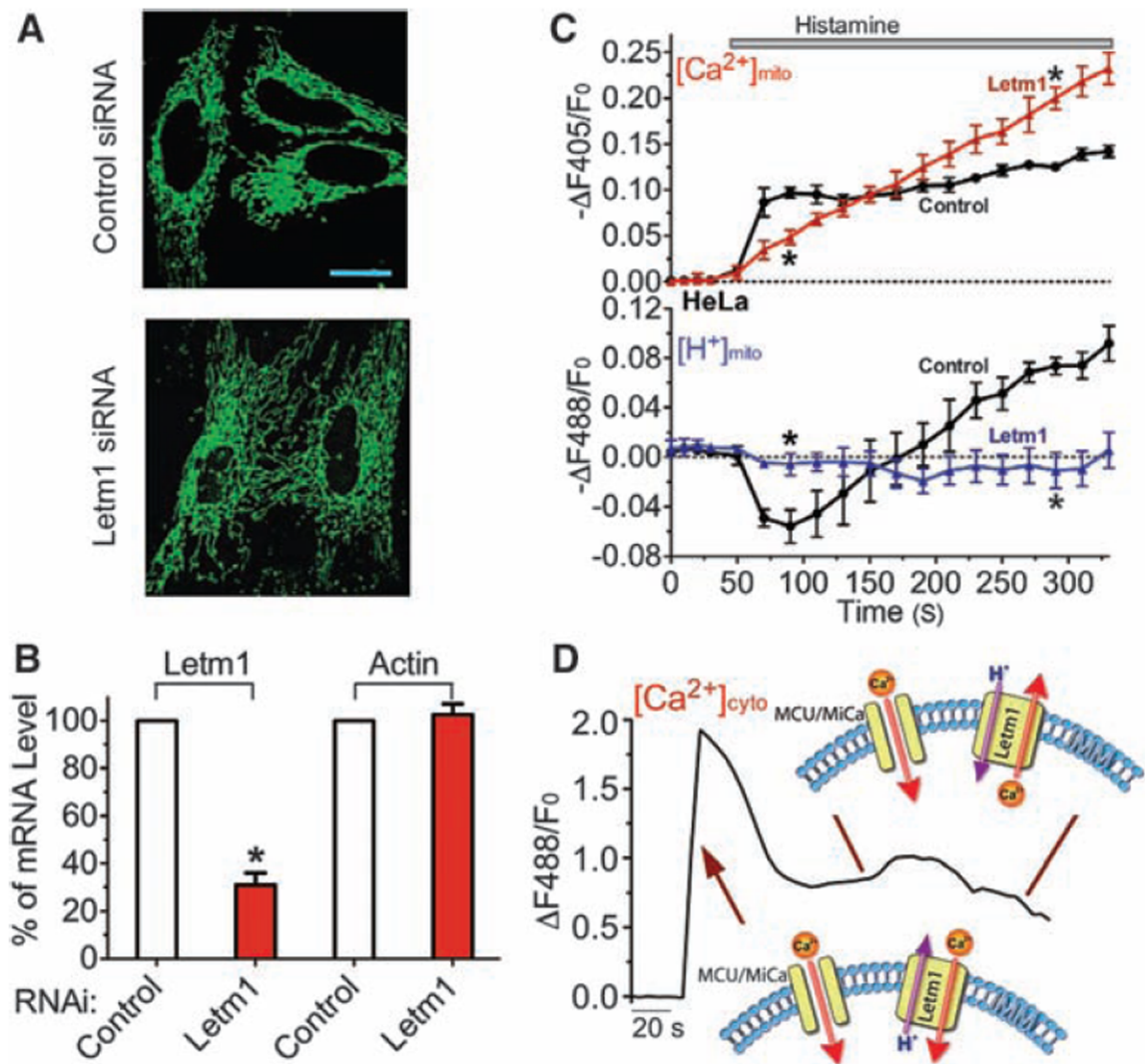


Fig. 3.

Letm1 knockdown disrupts Ca^{2+}/H^+ antiport in intact cells. **(A)** mt-Pericam-labeled mitochondria appear grossly normal in a representative image of *Letm1* siRNA-treated HeLa cells compared to cells treated with scrambled control siRNA. Scale bar: 20 μ m. **(B)** Determination of the mRNA level of *Letm1* and actin in control and *Letm1* siRNA-treated HeLa cells by quantitative RT-PCR ($n = 3$). **(C)** *Letm1* knockdown disturbs normal mitochondrial $[Ca^{2+}]_{mito}$ and $[H^+]_{mito}$ regulation in H1R-expressing HeLa cells. Histamine was applied to stimulate an increase in cytoplasmic $[Ca^{2+}]$ in cells in $[Ca^{2+}]_o = 2$ mM treated with control (circles; $n = 8$, 76 cells) or *Letm1* siRNAs (triangles; $n = 6$, 47 cells). Two independent *Letm1* siRNAs were used to confirm the result. **(D)** Representative trace of the $[Ca^{2+}]_{cyto}$ changes in HeLa cells upon histamine stimulation, and model of the roles of MCU/MiCa and Letm1 Ca^{2+}/H^+ exchanger activity under these conditions (arrows indicate their actions during the trace). All data shown are the mean \pm SEM (* $P < 0.05$, two-tailed Student's t test).

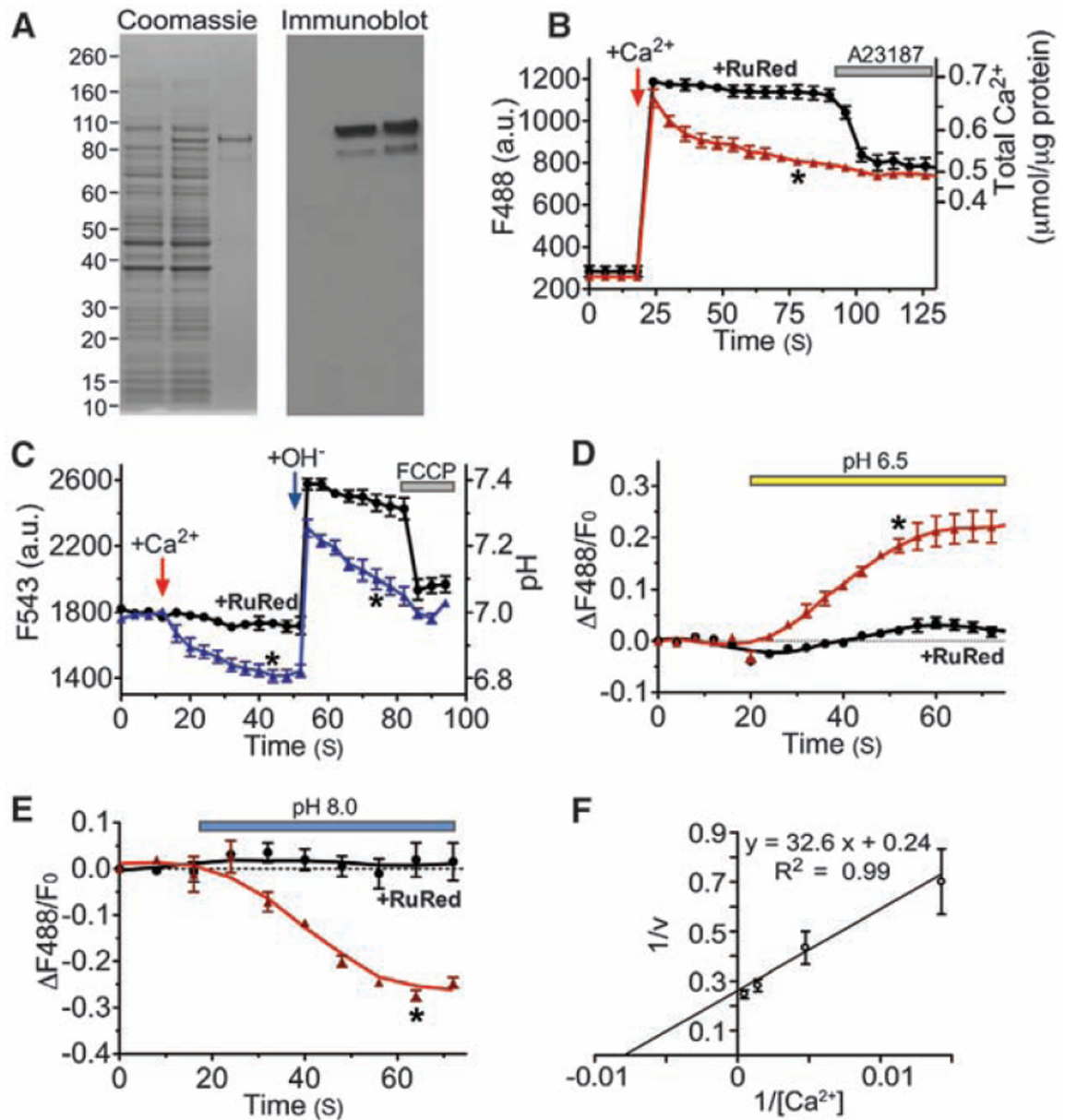


Fig. 4. Purified Letm1 reconstitutes Ca²⁺ transport in liposomes. **(A)** Letm1 protein stained by Coomassie blue (left) and antibody to His-Letm1 (right). Left lane, total bacterial cell lysate from control; middle lanes, Letm1-His-expressing bacteria; right lanes, isolated Letm1-His proteins. The band migrating at ~83 kD is consistent with Letm1's predicted molecular size. **(B)** Ca²⁺ addition initially increased external Ca²⁺, followed by Ca²⁺ import as indicated by decreasing fluorescence (triangles; $n = 8$). Ca²⁺ uptake was blocked by Ruthenium red (RuR; 10 nmol/μg; circles; $n = 5$), which was reversed by the Ca²⁺ ionophore, A23187 (5 μM). Liposomes occupied ~30% of the total volume based on the maximum Ca²⁺ uptake triggered by 4-Bromo-A23187. No leak was detected in liposomes without Letm1. **(C)** Ca²⁺-driven H⁺ efflux in Letm1 proteoliposomes. Addition of 100 μM Ca²⁺ triggered H⁺ efflux; application of 100 μM CsOH transiently increased the external pH, followed by a

rapid decline in pH (triangles; $n = 5$), which was blocked by RuR (10 nmol/ μg ; circles; $n = 3$). Finally, FCCP (10 μM , protonophore) reduced the external pH to basal levels. (D and E) pH-driven Ca^{2+} uptake in Letm1 proteoliposomes; Ca^{2+} release or uptake in Letm1 proteoliposomes was blocked by RuR. No-added-RuR, triangles, $n = 4$; 10 nmol/ μg RuR, circles, $n = 3$. (F) The inverse Ca^{2+} transport velocity ($1/v$; nmol/ μg protein per second) was plotted against inverse total added $[\text{Ca}^{2+}]$ (nmol/ μg protein, $n = 3$ to 8) in this double reciprocal plot to calculate K_m (137 nmol Ca^{2+} / μg protein) and V_{max} (4.2 nmol/ μg protein per second) using Michaelis-Menten assumptions (24). All data shown are the mean \pm SEM ($*P < 0.05$ in a two-tailed Student's t test).